

RAPID REPORT

Reduced mitochondrial coupling *in vivo* alters cellular energetics in aged mouse skeletal muscle

David J. Marcinek¹, Kenneth A. Schenkman^{3,4}, Wayne A. Ciesielski³, Donghoon Lee¹ and Kevin E. Conley^{1,2}

¹Department of Radiology, University of Washington Medical Center, Seattle, WA 98195, USA

²Departments of Physiology & Biophysics and Bioengineering, University of Washington Medical Center, Seattle, WA 98195, USA

³Children's Hospital and Regional Medical Center, Seattle, WA 98105, USA

⁴Departments of Pediatrics, Anaesthesiology and Bioengineering, University of Washington Medical Center, Seattle, WA 98195, USA

The mitochondrial theory of ageing proposes that the accumulation of oxidative damage to mitochondria leads to mitochondrial dysfunction and tissue degeneration with age. However, no consensus has emerged regarding the effects of ageing on mitochondrial function, particularly for mitochondrial coupling (P/O). One of the main barriers to a better understanding of the effects of ageing on coupling has been the lack of *in vivo* approaches to measure P/O. We use optical and magnetic resonance spectroscopy to independently quantify mitochondrial ATP synthesis and O₂ uptake to determine *in vivo* P/O. Resting ATP demand (equal to ATP synthesis) was lower in the skeletal muscle of 30-month-old C57Bl/6 mice compared to 7-month-old controls (21.9 ± 1.5 versus 13.6 ± 1.7 nmol ATP (g tissue)⁻¹ s⁻¹, $P = 0.01$). In contrast, there was no difference in the resting rates of O₂ uptake between the groups (5.4 ± 0.6 versus 8.4 ± 1.6 nmol O₂ (g tissue)⁻¹ s⁻¹). These results indicate a nearly 50% reduction in the mitochondrial P/O in the aged animals (2.05 ± 0.07 versus 1.05 ± 0.36 , $P = 0.02$). The higher resting ADP (30.8 ± 6.8 versus 58.0 ± 9.5 μmol g⁻¹, $P = 0.05$) and decreased energy charge (ATP/ADP) (274 ± 70 versus 84 ± 16 , $P = 0.03$) in the aged mice is consistent with an impairment of oxidative ATP synthesis. Despite the reduced P/O, uncoupling protein 3 protein levels were not different in the muscles of the two groups. These results demonstrate reduced mitochondrial coupling in aged skeletal muscle that alters cellular metabolism and energetics.

(Received 30 August 2005; accepted after revision 24 October 2005; first published online 27 October 2005)

Corresponding author D. J. Marcinek: Department of Radiology, University of Washington Medical Center, Seattle, WA 98195, USA. Email: dmarc@u.washington.edu

The mitochondrial theory of ageing proposes that oxidative damage to mitochondria leads to mitochondrial dysfunction and tissue degeneration with age (Miquel *et al.* 1980). Research into the effects of ageing on mitochondria has primarily focused on identifying oxidative damage and biochemical defects in the electron transport chain (ETC) in isolated mitochondria and cells. There is a striking lack of data on the effects of ageing *in vivo*, particularly data addressing the coupling of ATP synthesis to O₂ uptake (P/O). This is in spite of the fact that mitochondrial coupling is now recognized to be important in the integration of cell energetics (Nicholls, 2004), production of reactive oxygen species (ROS) (Brand, 2000; Nicholls, 2004), and cell death (Stoetzer *et al.* 2002; Heerdt *et al.* 2003) – all of which have been demonstrated to be important factors in the ageing process. The absence

of appropriate *in vivo* approaches is one of the primary reasons for this gap in our knowledge. This study uses a newly developed method to directly measure reduced mitochondrial coupling *in vivo* in aged mice.

Modulation of the P/O is primarily through changes in the proton leak through the inner mitochondrial membrane. An increase in proton leak reduces the ATP produced per O₂ consumed, thereby impairing the ability of the cell to meet the energetic demand of the tissue. The increased proton leak will also lead to reduced resting proton-motive force (Δp) (Brand, 2000), which has been demonstrated to sensitize the cell to the induction of apoptosis (Stoetzer *et al.* 2002; Heerdt *et al.* 2003). Evidence that oxidative damage to mitochondrial lipids increases proton leak (Brookes *et al.* 1998), and therefore more uncoupled respiration, suggests that increased

mitochondrial uncoupling may provide a link between the effects of age on oxidative damage, cellular energetics and cell death. This provides an additional mechanism, distinct from electron transport chain dysfunction, for the role of mitochondria in loss of function and degeneration with age.

Due to a lack of appropriate *in vivo* approaches, the relatively few groups (in relation to those measuring mtDNA damage and ETC dysfunction) that have addressed mitochondrial proton leak in ageing tissues have done so in isolated mitochondria and cells. Functional assays performed in isolated organelles and cells may not reflect *in vivo* function because mitochondrial coupling and proton leak are modulated by many cellular factors (e.g. flux rates, oxygenation, metabolite levels) (Gnaiger *et al.* 2000) and damage to mitochondria can occur during the isolation process (Anson *et al.* 2000). We suggest that a direct *in vivo* measurement of mitochondrial P/O is the necessary next step to understand the role of proton leak and reduced coupling in the degenerative pathologies of ageing.

This work implements a strategy that combines the physiological relevance of *in vivo* analysis with the ability to measure mitochondrial coupling. We use a combination of optical and magnetic resonance techniques developed in our laboratories to independently measure O₂ and ATP fluxes in intact skeletal muscle (Marcinek *et al.* 2004). This approach allows us not only to determine the effects of age on mitochondrial coupling, but also to determine how reduced coupling affects *in vivo* energetics and resting metabolism. We find significantly lower P/O in aged mouse skeletal muscle associated with a decrease in resting ATP demand and a lower ATP/ADP. These results indicate that reduced mitochondrial efficiency significantly alters the bioenergetics and metabolism in ageing skeletal muscle.

Methods

Animals

All experiments were approved by the Animal Care and Use Committee of the University of Washington. Female 30-month-old C57Bl/6 mice ($n = 6$, 23.5 ± 1.3 g, mean \pm s.e.m.) were purchased from the aged rodent colony of the National Institute on Ageing. Due to the genetic contamination of the NIA colony, the 7-month-old C57Bl/6 mice were purchased from Jackson Laboratories ($n = 6$, 27.1 ± 1.4 g). This strain was used to derive the NIA colony. Mice were anaesthetized with an intraperitoneal injection of 2,2,2-tribromoethanol (0.55 mg (g body wt)⁻¹) in saline (5% v/v). Respiration rate was monitored throughout the experiments and supplemental anaesthetic was given subcutaneously as needed. Animals were allowed to recover from anaesthesia overnight between optical and MRS experiments. The order in which

the optical and MRS measurements were performed was varied in each group to ensure that there was no effect of experimental order on the measured variables.

For the optical experiments, the hair was removed from the lower hindlimb using a commercial hair removal cream (Neet®). The leg was secured between the fibre optic bundles by fixing the ankle and foot in place such that light travelled through the leg distal to the knee. During the optical experiments the animals breathed 100% O₂ to maintain high Hb saturation of the blood. For the MRS experiments, the leg was secured in the same manner so that the entire volume of the hindlimb musculature was sampled. Ischaemia was induced during both optical and MRS experiments either by suspending a 0.5-kg weight from a 3.2-mm cord wrapped around the leg or inflating a custom built cuff around the leg to 200 mmHg. The durations of ischaemia – 7 min for optical and 10 min for MRS – were well below the 3 h threshold demonstrated to result in tissue damage in limb skeletal muscle (Blaisdell, 2002). The animals were kept warm with forced air throughout the experiments and tissue sampling to maintain the temperature of the leg at $37 \pm 0.5^\circ\text{C}$. After the final spectra were acquired, the hindlimb was removed under anaesthesia, and frozen between aluminium blocks at liquid N₂ temperature. The animals were then killed with an overdose of anaesthetic given intraperitoneally.

Optical spectroscopy and analysis

Optical spectra were collected between 450 and 950 nm as previously described (Marcinek *et al.* 2003). Partial least-squares (PLS) analysis was used to determine the Hb and Mb saturations from the optical spectra of the mouse leg. This analysis has been applied to skeletal muscle *in vivo* (Marcinek *et al.* 2003, 2004) and cardiac muscle *in situ* (Schenkman, 2001). Weighting coefficients corresponding to known Hb or Mb saturation values are generated for each wavelength (560–850 nm) using an *in vitro* calibration set. These weighting coefficients are applied to the *in vivo* spectra to determine the saturation of either Hb or Mb in the mouse hindlimb. Second derivative spectra are used in the PLS analysis to remove the effect of baseline offsets.

Calibration sets for PLS analysis of the mouse hindlimb were constructed as previously described (Marcinek *et al.* 2003). Briefly, the spectra of oxy- and deoxy-Hb and Mb and oxidized and reduced cytochrome *c* in scattering media are collected. Oxy and deoxy spectra of each absorber are mathematically added in different proportions to generate composite spectra that span the range of saturation and redox states for each absorber. Concentrations of each absorber are optimized such that the composite spectra approximate the *in vivo* spectra. Weighting coefficients from one calibration set are used to predict the saturations of a second set to determine the

accuracy of the PLS algorithm in predicting unknown Hb and Mb saturations. The prediction errors were found to be 4.6% and 7.4% for Hb and Mb, respectively (Marcinek *et al.* 2003). Tissue Hb and Mb concentrations were determined for each animal by SDS-PAGE analysis as in Marcinek *et al.* (2003).

³¹P MRS

The magnetic resonance experiments were performed in either in a 4.7 tesla (T) Bruker horizontal bore magnet or Oxford 7.0 T vertical bore magnet. The mouse body was orientated horizontally and the leg pulled through a three-turn solenoidal coil with an inner diameter of 8 mm and a length of 6 mm tuned to ³¹P resonance frequency (81.15 MHz at 4.7 T and 121.65 at 7 T). In the vertical bore 7 T magnet the mouse head and body were suspended horizontally from flexible straps above the coil. B₀ field homogeneity was optimized by shimming using the proton peak from tissue water. Unfiltered PCr line widths were 20–30 Hz. A high signal-to-noise ³¹P MRS spectrum was taken under fully relaxing conditions – 128 acquisitions, 16 s interpulse delay, 3500 Hz spectral width, 1024 data points at 4.7 T and 16 acquisitions, 16 s interpulse delay, 5000 Hz spectral width, 2048 data points at 7 T. Dynamic spectra were acquired during the rest–ischaemia–recovery experiment with a standard one-pulse sequence with a 1.5 s interpulse delay and a 45 deg flip angle. For each dynamic spectrum, 16 free induction decays were added to obtain higher signal to noise spectra with a resolution of 26 s (sum of acquisition time and time to write data). The fully relaxed and dynamic free induction decays were Fourier transformed, baseline corrected, line broadened with a 10 Hz exponential filter, and zero-filled. Fully relaxed peak areas were calculated by integration of the processed spectra using the Omega software on a General Electric console for the 4.7 T experiments and VNMR software on a Varian Inova console for the 7 T experiments. Peak areas relative to a standard spectrum were determined from the dynamic spectra with the Fit to Standard algorithm (Heineman *et al.* 1990).

Calculations

Resting ATP and total creatine concentrations in the 7- and 30-month-old mice were measured by HPLC analysis (Wiseman *et al.* 1992) of extracts from frozen hind-limbs. Resting metabolite concentrations were expressed per volume cell water assuming 0.7 ml intracellular water per gram muscle (Sjogaard & Saltin, 1982) to ease comparison with published values, while ATP and O₂ fluxes were expressed in nmol (g tissue)⁻¹ s⁻¹. Resting PCr concentrations were calculated using the PCr to γ -ATP peak ratio from the fully relaxed spectra and the mean

ATP concentrations for each group. PCr concentrations throughout the dynamic experiments were determined by comparing the relative peak areas with the resting PCr concentrations. The chemical shift of P_i relative to PCr in each spectrum was used to calculate pH (Taylor *et al.* 1983).

Resting ADP concentrations were calculated by rearranging the equation for the creatine kinase equilibrium constant (K_{CK}):

$$[ADP] = ([ATP][Cr])/([PCr]K_{CK}) \quad (1)$$

where PCr, ATP, and Cr concentrations are determined as described above. K_{CK} was adjusted for pH and free Mg²⁺ concentration of 0.6 mM (Golding *et al.* 1995).

Resting O₂ consumption and ATP synthesis

The resting rates of ATP synthesis and O₂ consumption were determined during brief ischaemic bouts (Marcinek *et al.* 2004). Here we present a brief description of the approach. In the absence of blood flow the O₂ content of the tissue is the product of the O₂ saturation of Hb and Mb and their concentrations plus the small amount of dissolved O₂. Mitochondrial O₂ consumption can be determined by following the decline in O₂ saturation of Hb and Mb. Once the tissue is nearly anoxic oxidative phosphorylation ceases and PCr is consumed to meet the ATP demand. Prior to the onset of glycolytic ATP synthesis (Marcinek *et al.* 2004), this rate of PCr breakdown measures the rate of mitochondrial ATP synthesis (Blei *et al.* 1993).

Western blots

Muscle homogenates were prepared for electrophoretic separation and Western blotting as previously described (Marcinek *et al.* 2003). Three hundred and seventy-five micrograms of homogenized muscle tissue per lane was separated on a 10% Tris–glycine gel (Bio-Rad, Hercules, CA, USA). Proteins were transferred to 0.2 μ m nitrocellulose membranes (Bio-Rad) and blocked in 3% gelatin in Tris-buffered saline (TBS) for 1 h. at room temperature. Blots were incubated overnight at 4°C with rabbit anti-human uncoupling protein (UCP) 3 (1 : 3000) (UCP3-2, Alpha Diagnostics, San Antonio, TX, USA). The specificity of this antibody for UCP3 in mouse muscle has been verified using UCP3 knockout mice (Jimenez *et al.* 2002). Blots were then washed 2 \times 5 min in 0.05% Tween–TBS (TTBS) and incubated for 2 h in goat anti-rabbit alkaline phosphatase conjugate secondary antibody (Bio-Rad). After 2 \times 5 min TTBS and 1 \times 5 min TBS washes the signal was detected according to the Bio-Rad Alkaline Phosphatase Conjugate Substrate Kit. Membranes were photographed using a

digital camera and quantified with NIH Image software on a Macintosh computer (developed at the US National Institutes of Health and available on the Internet at <http://rsb.info.nih.gov/nih-image/>). UCP3 bands were normalized to control bands on each gel. Preliminary tests were performed to ensure that the UCP3 signal reflected different amounts of UCP3 protein in the band.

Data analysis

All statistical analyses were conducted using GraphPad Prism version 3.0a software for the Macintosh (GraphPad Software, Inc., San Diego, CA, USA). ATPase and O₂ consumption rates were determined from the slopes of the least-square regression lines through the plots of PCr concentrations and total O₂ stores during ischaemia, respectively. Student's two-tailed *t* test was used for all comparisons between the 7- and 30-month-old mice. Data are presented as means ± standard error of the mean. Significance was defined as *P* < 0.05.

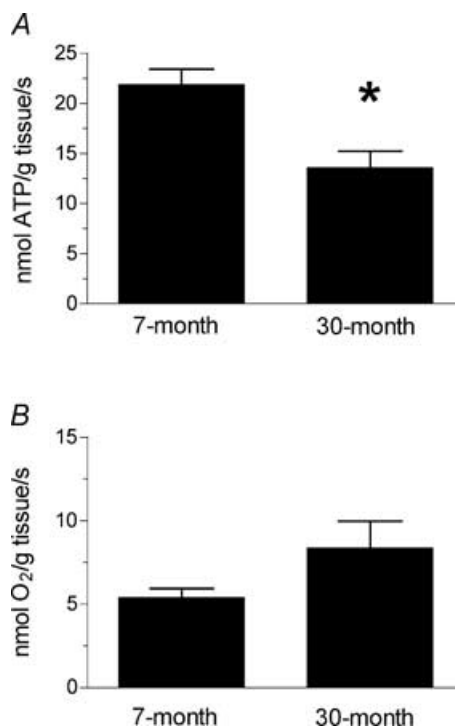


Figure 1. Resting metabolism in 7- and 30-month-old mouse skeletal muscle

A, the hindlimb muscles from the aged (30-month-old) mice have a significantly reduced resting ATP demand compared to the adult (7-month-old) controls (**P* < 0.05). B, there is no difference in the resting rate of O₂ consumption in the hindlimb muscles of the control (*n* = 6) and aged mice, despite the different ATP demand shown in Fig. 1A. *n* = 5 except where noted.

Results

Reduced mitochondrial coupling

In vivo mitochondrial function is qualitatively different in the skeletal muscles of adult and 30-month-old mice. Figure 1A demonstrates that the resting ATP demand is more than 30% lower in aged muscles, while the rate of resting O₂ consumption is not significantly different in the two groups (Fig. 1B). Resting muscle is in energy balance so this reduced ATP demand reflects a reduced rate of mitochondrial ATP synthesis. The lower rates of ATP synthesis without a difference in O₂ uptake rates indicate partial uncoupling of oxidative phosphorylation in the aged muscles. The P/O values in the skeletal muscle from the aged mice shown in Fig. 2 are more than 50% lower than found in the muscle of adult mice. These results indicate that the aged mice produce fewer ATP per O₂ consumed by the leg muscles.

Altered cell energetics

We found significantly elevated ADP concentrations and reduced ATP/ADP and PCr concentrations with age (Table 1). Resting pH was also lower in the aged muscles. All of these metabolites are linked through the creatine kinase reaction and represent a shift toward lower resting ATP concentrations in the aged mouse muscle. In support of this view, we found that ATP concentrations in the aged mice tended to be lower, but not significantly, than in the adults controls.

No change in UCP3 expression

To address whether increased proton leak in the aged tissues is due to an up-regulation of UCP3 expression, we determined the UCP3 protein content in muscle homogenates from the same tissues in which we made the physiological measurements. Figure 3 demonstrates that

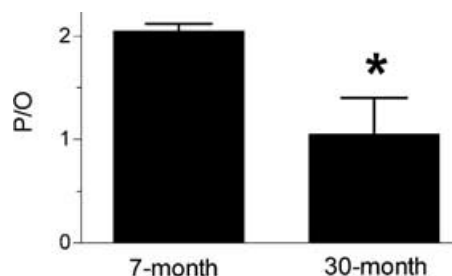


Figure 2. P/O values for 7- and 30-month-old mouse skeletal muscle

The P/O is significantly reduced in the 30-month-old (*n* = 5) compared to the 7-month-old animals (*n* = 5) (**P* < 0.05).

Table 1. Values for metabolites from 7- and 30-month-old mouse hindlimb muscles

	7-month	30-month	P-value
ATP (mM)	6.88 ± 0.79	4.16 ± 1.01	0.09
PCr/ATP	3.37 ± 0.11	3.83 ± 0.33	NS
pH	7.13 ± 0.04	6.99 ± 0.03*	0.03
TCr (mM)	37.1 ± 3.3	37.5 ± 0.7	NS
PCr (mM)	22.4 ± 0.7	16.2 ± 1.3*	< 0.01
ADP (μM)	30.8 ± 6.8	58.0 ± 9.5*	0.05
ATP/ADP	275 ± 70	84 ± 16*	0.03

The first three variables were measured directly using either HPLC (ATP and TCr) or MRS (PCr/ATP and pH). The final four variables were derived as described in the methods. *P*-values were determined using a two-tailed unpaired *t* test. *n* = 5 for all values except 7-month-old ATP where *n* = 6.

UCP3 expression is not significantly different in the hindlimbs of the adult and aged mice.

Discussion

This work provides a direct measurement of changes in cell energy fluxes and the coupling of oxidative phosphorylation (*P/O*) with age *in vivo*. Surprisingly, we find a significant decrease in the resting ATP demand (and therefore ATP synthesis rate) with no change in the rate of O₂ uptake in the aged muscles. The net result of this is a 50% reduction in the mitochondrial *P/O* in muscle of aged mice.

Resting metabolism

Independent measurements of O₂ consumption and ATPase rates provide information on resting metabolism not available with other approaches. Resting metabolism is an important variable in understanding the effect of age on cells because this state reflects the major part of the energy budget of skeletal muscle and the energetic demand for maintenance functions, including molecular turnover and ion transport. Lower ATPase rates in the aged mouse hindlimb support other work indicating a reduction in protein synthesis (Rooyackers *et al.* 1996) and impairment of mitochondrial degradation (Kowald & Kirkwood, 2000), both of which would contribute to a reduced resting ATP demand. With reduced molecular turnover in ageing cells oxidative damage to macromolecules would accumulate to a greater extent than in adult tissues and could explain the changes in mitochondrial function described herein.

Down-regulation of metabolism with age may itself lead to pathological conditions. For example, lower resting ATP demand in elderly human muscle has been found in muscles with an accumulation of intramyocellular lipids and insulin resistance (Petersen *et al.* 2003). However,

this earlier study also found a decline in TCA cycle flux and concluded that O₂ uptake declined in parallel to ATP synthesis in elderly muscle. This concomitant decline in O₂ and ATP fluxes indicates a reduced resting metabolic rate in elderly human muscle, but not necessarily mitochondrial dysfunction. In contrast, no difference in O₂ uptake in mouse skeletal muscle in this study indicates increased proton leak and mitochondrial uncoupling.

Reduced mitochondrial coupling

The significance of the *in vivo* measurements is that they provide direct evidence of reduced mitochondrial coupling under physiological O₂ tensions and ATP flux rates. Our results provide strong evidence that reduced mitochondrial coupling contributes to the impairment of oxidative phosphorylation in aged mouse skeletal muscle. There is currently a lack of consensus regarding proton leak and mitochondrial coupling in ageing tissues. Previous investigations in isolated mitochondria have found evidence for increased (reviewed by Harper *et al.* 2004), unchanged (Rasmussen *et al.* 2003), or decreased (Kerner *et al.* 2001) proton leak in aged skeletal muscle. The disparate results *in vitro* are likely to be due to methodological differences in the isolation or assay conditions employed by each group. Work on isolated mitochondria typically measures mitochondrial respiration under state 3 or state 4 conditions or after inhibiting the F₁F₀ ATPase. These approaches provide detailed biochemical analysis of mitochondrial function, but the assay conditions are inherently non-physiological (Marcinek, 2004). Since mitochondrial function has been shown to be sensitive to assay conditions and flux rates (Gnaiger *et al.* 2000), extrapolating results from non-physiological conditions to *in vivo* function is problematic. The data presented here support the *in vitro* studies that have shown increases in proton leak with age. Although age is the most likely candidate, other causes for the differences in mitochondrial function are possible due to potential differences in the life histories of the two

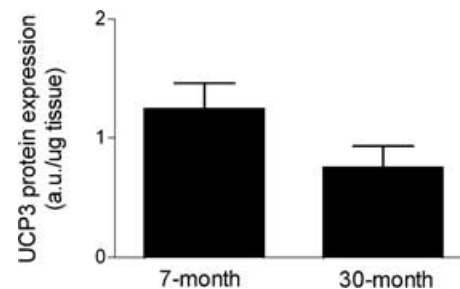


Figure 3. UCP3 protein expression in 7- and 30-month-old mouse skeletal muscle

UCP3 protein levels between the 7- and 30-month-old mouse hindlimbs are not significantly different. *n* = 6 for both groups.

groups of C57Bl/6 mice. Nonetheless, our *in vivo* results provide a critical link between work in isolated systems and mitochondrial function in the intact organism.

Reduced mitochondrial efficiency significantly alters the bioenergetics of skeletal muscle in the 30-month-old mice. This shift in cellular energetics is due both to a reduction in the number of ATP produced per O₂ consumed as well as a thermodynamic limitation on the ATP/ADP that can be maintained by the cell. The limitation is due to a lower Δp across the inner mitochondrial membrane caused by greater proton leak associated with the reduced coupling in the aged skeletal muscle. The reduced Δp will limit the ATP/ADP that can be maintained by oxidative phosphorylation due to the equilibrium relationship between Δp and the ATP/ADP of the cell (Nicholls, 2004). These predictions are consistent with the higher resting ADP and lower ATP/ADP we observe in the aged skeletal muscle. The end result of this shift in energetics is that resting ADP concentrations are nearly double in the aged muscle despite the 50% reduction in the rate of ATP synthesis.

Reduced coupling may have an impact on ageing muscle beyond the direct effects on cell energetics. Lower Δp itself may contribute to the loss of muscle fibres and sarcopenia. Reduced Δp has been shown to reduce the threshold for the mitochondrial permeability transition (MPT) (Bernardi, 1992), which induces apoptosis by releasing cytochrome *c* into the cytoplasm. This effect on the MPT supports the results demonstrating that increased rates of apoptosis are associated with an increase in proton conductance in multiple cell types (Stoetzer *et al.* 2002; Heerdt *et al.* 2003). Therefore, the increased proton leak in the 30-month-old mouse muscle could lead to hotspots of apoptosis along the muscle fibres and be another mechanism leading to segmental atrophy and fibre loss described by Aiken and coworkers in ageing skeletal muscle (McKenzie *et al.* 2002).

Uncoupling proteins

One hypothesis suggests that increased proton leak is an adaptive response in ageing animals to reduce Δp and attenuate reactive oxygen species (ROS) production, particularly at the complex I–ubiquinone interface (Brand, 2000). The proposed mechanism is an increased proton conductance due to uncoupling protein activity. This UCP mediated leak may be through direct transport of protons or indirectly as a by-product of fatty acid translocation across the mitochondrial inner membrane (Garlid *et al.* 2001). Our results indicate that the mitochondrial uncoupling that we observe in aged mouse skeletal muscle is not mediated by increased protein expression of the muscle specific uncoupling protein isoform, UCP3. It has recently been observed that oxidative stress may play a role in regulating UCP function *in vitro*

(Echtay *et al.* 2002). Our results do not address the potential up-regulation of UCP3 proton translocating activity by ROS or by-products of oxidative damage in the aged mice. However, this hypothesis proposes mild uncoupling of oxidative phosphorylation as a protective mechanism against ROS production as opposed to the severe uncoupling measured in this study. UCP3 activity may reduce ROS production at younger ages and thus delay the accumulation of oxidative damage, but we suggest that at the old age examined in this study oxidative damage accumulates, leading to further increases in proton leak and mitochondrial dysfunction. Future studies that combine *in vivo* measurements of mitochondrial function with genetic manipulations of uncoupling proteins and antioxidant defenses will be necessary to sort out the mechanisms underlying the changes in mitochondrial function in the aged mice.

References

- Anson RM, Hudson E & Bohr VA (2000). Mitochondrial endogenous oxidative damage has been overestimated. *FASEB J* **14**, 355–360.
- Bernardi P (1992). Modulation of the mitochondrial cyclosporin A-sensitive permeability transition pore by the proton electrochemical gradient. Evidence that the pore can be opened by membrane depolarization. *J Biol Chem* **267**, 8834–8839.
- Blaisdell FW (2002). The pathophysiology of skeletal muscle ischemia and the reperfusion syndrome: a review. *Cardiovasc Surg* **10**, 620–630.
- Blei ML, Conley KE & Kushmerick MJ (1993). Separate measures of ATP utilization and recovery in human skeletal muscle. *J Physiol* **465**, 203–222.
- Brand MD (2000). Uncoupling to survive? The role of mitochondrial inefficiency in ageing. *Exp Gerontol* **35**, 811–820.
- Brookes PS, Land JM, Clark JB & Heales SJ (1998). Peroxynitrite and brain mitochondria: evidence for increased proton leak. *J Neurochem* **70**, 2195–2202.
- Echtay KS, Roussel D, St-Pierre J, Jekabsons MB, Cadenas S, Stuart JA *et al.* (2002). Superoxide activates mitochondrial uncoupling proteins. *Nature* **415**, 96–99.
- Garlid KD, Jaburek M & Jezek P (2001). Mechanism of uncoupling protein action. *Biochem Soc Trans* **29**, 803–806.
- Gnaiger E, Méndez G & Hand SC (2000). High phosphorylation efficiency and depression of uncoupled respiration in mitochondria under hypoxia. *Proc Natl Acad Sci U S A* **97**, 11080–11085.
- Golding EM, Teague WE Jr & Dobson GP (1995). Adjustment of *K'* to varying pH and pMg for the creatine kinase, adenylate kinase and ATP hydrolysis equilibria permitting quantitative bioenergetic assessment. *J Exp Biol* **198**, 1775–1782.
- Harper ME, Bevilacqua L, Hagopian K, Weindruch R & Ramsey JJ (2004). Ageing, oxidative stress, and mitochondrial uncoupling. *Acta Physiol Scand* **182**, 321–331.

- Heerdt BG, Houston MA, Wilson AJ & Augenlicht LH (2003). The intrinsic mitochondrial membrane potential ($\Delta\psi_m$) is associated with steady-state mitochondrial activity and the extent to which colonic epithelial cells undergo butyrate-mediated growth arrest and apoptosis. *Cancer Res* **63**, 6311–6319.
- Heineman FW, Eng J, Berkowitz BA & Balaban RS (1990). NMR spectral analysis of kinetic data using natural lineshapes. *Mag Res Med* **13**, 490–497.
- Jimenez M, Yvon C, Lehr L, Leger B, Keller P, Russell A *et al.* (2002). Expression of uncoupling protein-3 in subsarcolemmal and intermyofibrillar mitochondria of various mouse muscle types and its modulation by fasting. *Eur J Biochem* **269**, 2878–2884.
- Kerner J, Turkaly PJ, Minkler PE & Hoppel CL (2001). Aging skeletal muscle mitochondria in the rat: decreased uncoupling protein-3 content. *Am J Physiol Endocrinol Metab* **281**, E1054–E1062.
- Kowald A & Kirkwood TB (2000). Accumulation of defective mitochondria through delayed degradation of damaged organelles and its possible role in the ageing of post-mitotic and dividing cells. *J Theor Biol* **202**, 145–160.
- McKenzie D, Bua E, McKiernan S, Cao Z & Aiken JM (2002). Mitochondrial DNA deletion mutations: a causal role in sarcopenia. *Eur J Biochem* **269**, 2010–2015.
- Marcinek DJ (2004). Mitochondrial dysfunction measured in vivo. *Acta Physiol Scand* **182**, 343–352.
- Marcinek DJ, Ciesielski WA, Conley KE & Schenkman KA (2003). Oxygen regulation and limitation to cellular respiration in mouse skeletal muscle in vivo. *Am J Physiol Heart Circ Physiol* **285**, H1900–H1908.
- Marcinek DJ, Schenkman KA, Ciesielski WA & Conley KE (2004). Mitochondrial coupling in vivo in mouse skeletal muscle. *Am J Physiol Cell Physiol* **286**, 457–463.
- Miquel J, Economos AC, Fleming J & Johnson JE Jr (1980). Mitochondrial role in cell aging. *Exp Gerontol* **15**, 575–591.
- Nicholls DG (2004). Mitochondrial membrane potential and aging. *Aging Cell* **3**, 35–40.
- Petersen KF, Befroy D, Dufour S, Dziura J, Ariyan C, Rothman DL *et al.* (2003). Mitochondrial dysfunction in the elderly: possible role in insulin resistance. *Science* **300**, 1140–1142.
- Rasmussen UF, Krstrup P, Kjaer M & Rasmussen HN (2003). Experimental evidence against the mitochondrial theory of aging. A study of isolated human skeletal muscle mitochondria. *Exp Gerontol* **38**, 877–886.
- Rooyackers OE, Adey DB, Ades PA & Nair KS (1996). Effect of age on in vitro rates of mitochondrial protein synthesis in human skeletal muscle. *Proc Natl Acad Sci U S A* **93**, 15364–15369.
- Schenkman KA (2001). Cardiac performance as a function of intracellular oxygen tension in buffer-perfused hearts. *Am J Physiol Heart Circ Physiol* **281**, H2463–H2472.
- Sjogaard G & Saltin B (1982). Extra- and intracellular water spaces in muscles of man at rest and with dynamic exercise. *Am J Physiol* **243**, R271–R280.
- Stoetzer OJ, Pogrebniak A, Pelka-Fleischer R, Hasmann M, Hiddemann W & Nuessler V (2002). Modulation of apoptosis by mitochondrial uncouplers: apoptosis-delaying features despite intrinsic cytotoxicity. *Biochem Pharmacol* **63**, 471–483.
- Taylor DJ, Bore PJ, Styles P, Gadian DG & Radda GK (1983). Bioenergetics of intact human muscle a ^{31}P nuclear resonance study. *Mol Biol Med* **1**, 77–94.
- Wiseman RW, Moerland TS, Chase PB, Stuppard R & Kushmerick MJ (1992). High-performance liquid chromatographic assays for free and phosphorylated derivatives of the creatine analogues BETA-guanidopropionic acid and 1-carboxy-methyl-2-iminoimidazolidine (cyclocreatine). *Anal Biochem* **204**, 383–389.

Acknowledgements

This work has benefited from numerous discussions with Dr Martin Kushmerick and from his critical reading of the manuscript. We also thank Rudy Stuppard and Dr Eric Shankland for their technical assistance. This work was supported by NIH Grants AR-36281, AG-00057 and AG-22385 and a Nathan Shock Pilot Project Award.